Electronic Supplementary Information

Metal-Organic Framework-Derived Pseudocapacitive Titanium Oxide/Carbon Core/Shell Heterostructure for High Performance Potassium Ion Hybrid Capacitor

Hongxia Li,[a,b,c] Jiangtao Chen,[a] Li Zhang,[a] Kunjie Wang,[c] Xu Zhang,[a] Bingjun Yang,[a,b] Lingyang Liu,[a,b] Weisheng Liu,[d] Xingbin Yan*[,a,b,e]

[a] Laboratory of Clean Energy Chemistry and Materials, State Key Laboratory of Solid Lubrication, Lanzhou Institute of Chemical Physics, Chinese Academy of Sciences, Lanzhou 730000, China

[b] Center of Materials Science and Optoelectronics Engineering, University of Chinese Academy of Sciences, Beijing 100049, China

[c] School of Petrochemical Engineering, Lanzhou University of Technology, Lanzhou 730050, P. R. China

[d] College of Chemistry and Chemical Engineering, Lanzhou University, Lanzhou 730000, P. R. China.

[e] Dalian National Laboratory for Clean Energy, Chinese Academy of Sciences, Dalian 116000, China

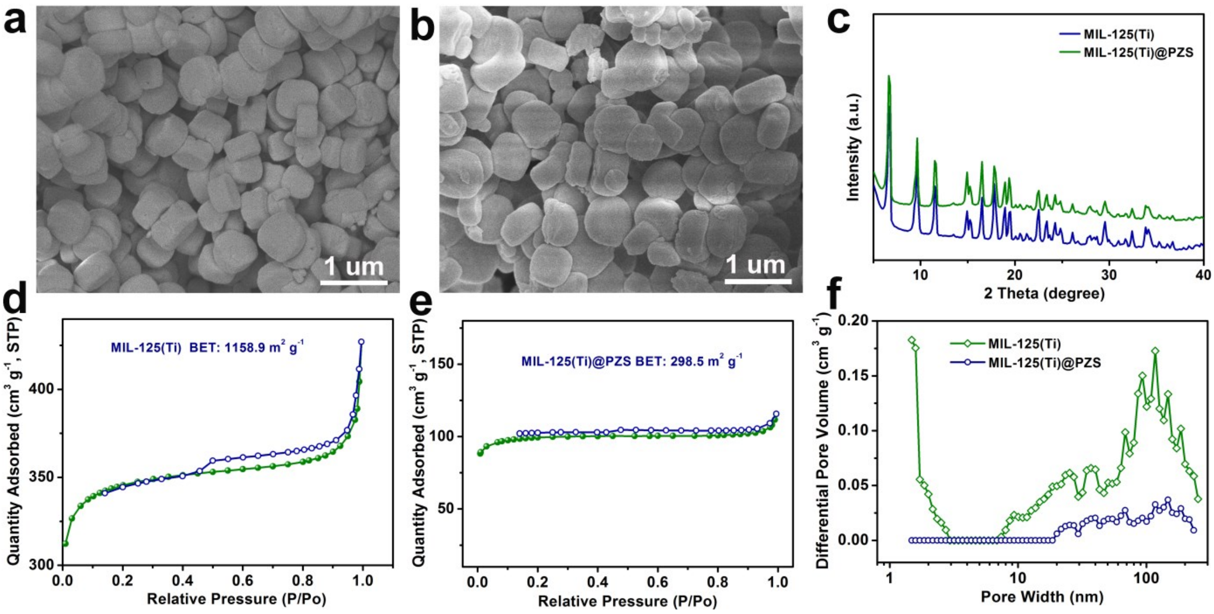

Fig. S1. Morphology and structure characterization: (a) SEM image of MIL-125 (Ti), (b) SEM image of MIL-125 (Ti)@PZS, (c) XRD patterns of MIL-125 (Ti) and MIL-125 (Ti)@PZS. Nitrogen absorption/desorption isotherm curves of (d) MIL-125 (Ti), (e) MIL-125 (Ti)@PZS. (f) The corresponding pore size distribution curves.

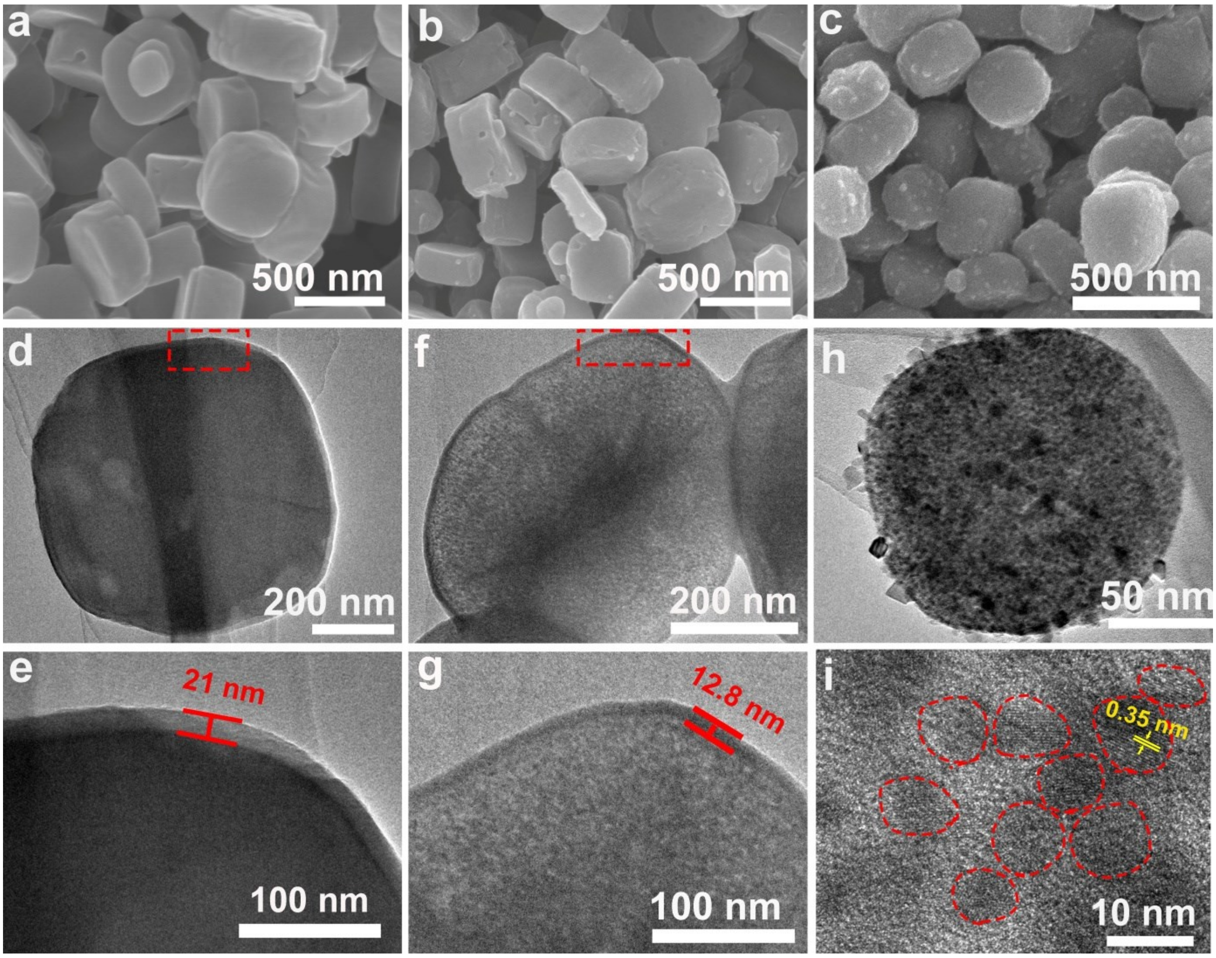

Fig. S2 Morphology characterization: SEM images of (a) TiO_2/C@NPSC-600, (b) TiO_2/C@NPSC-800 and (c) TiO_2/C-700. TEM images of (d, e) MIL-125(Ti)@PZS, (f, g, i) TiO_2/C@NPSC-700 and (h) TiO_2/C-700.

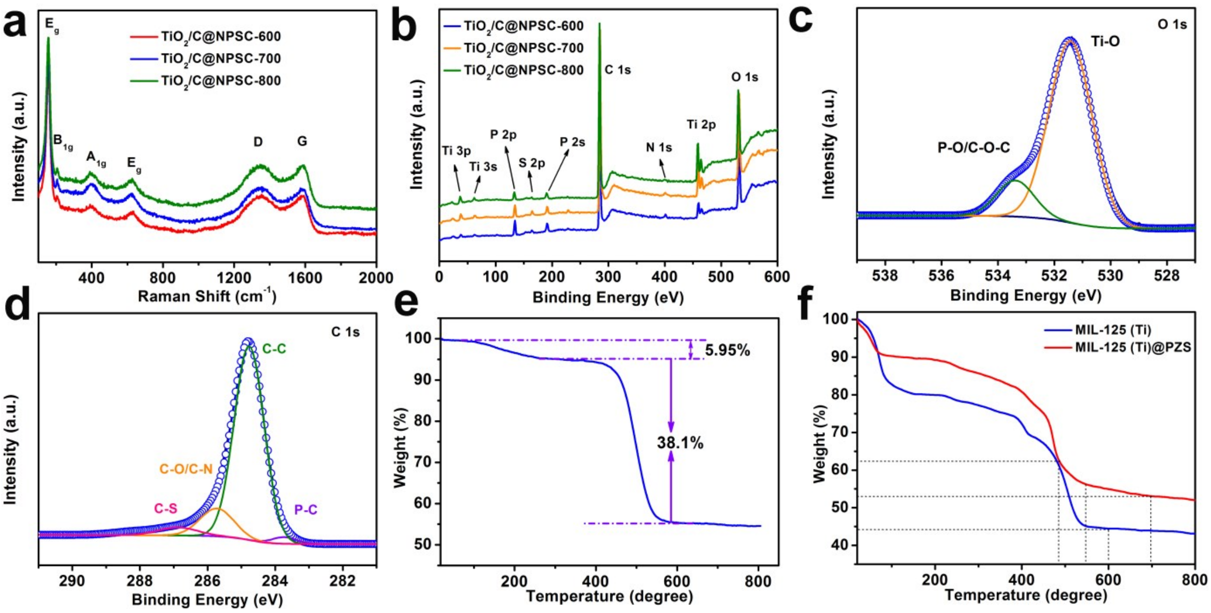

Fig. S3 (a) Raman spectra and (b) XPS full surveys of TiO_2/C@NPSC-x. (c) O 1s spectra, (d) C 1s spectra, (e) TG curve of TiO_2/C@NPSC-700 in air. (f) TG curves of MIL-125 (Ti)@PZS and MIL-125 (Ti) tested in N_2 atmosphere (as shown in TG curves, before 500 °C, the weight loss trends were similar in both MIL-125 (Ti) and MIL-125 (Ti)@PZS because only the decomposition of MOFs precursor was occurred. In comparison, the PZS layer decomposition resulted in the discrepancy of TG curves between MIL-125 (Ti)@PZS and MIL-125 (Ti) when the annealing temperature was higher than 500 °C).

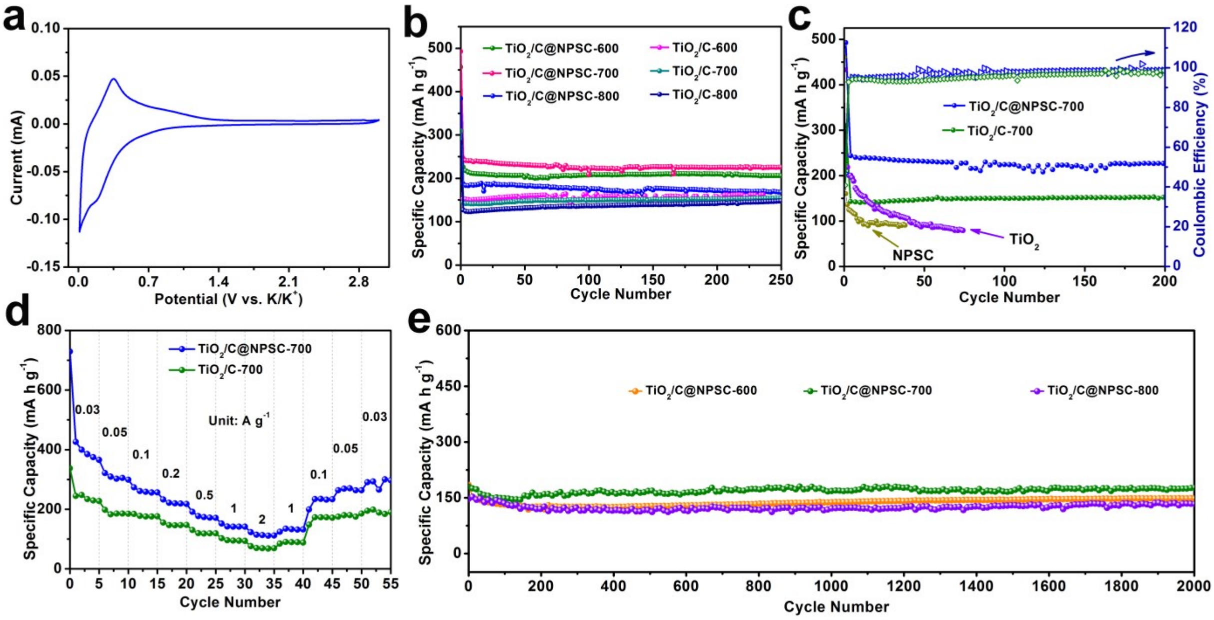

Fig. S4 (a) CV curve of acetylene carbon black at scan rate of 0.1 mV s^{-1}. (b) The cycling performance of TiO_2/C@NPSC-x compared with TiO_2/C-x (prepared by pyrolysis of MIL-125 (Ti)) at 0.1 A g^{-1}. (c) The comparison of electrochemical performance of TiO_2/C@NPSC-700, TiO_2/C-700, anatase TiO_2 and NPSC at 0.1 A g^{-1}, in where, TiO_2 was prepared by pyrolyzing of TiO_2/C@NPSC-700 at 500 °C in air, NPSC (N, P, S-doped carbon) was derived from pyrolysis of PZS polymer. (d) rate capability at different current densities ranging from 0.03 to 2 A g^{-1} of TiO_2/C@NPSC-700 and TiO_2/C-700. (e) The cycling performance of TiO_2/C@NPSC-x at 0.5 A g^{-1}.

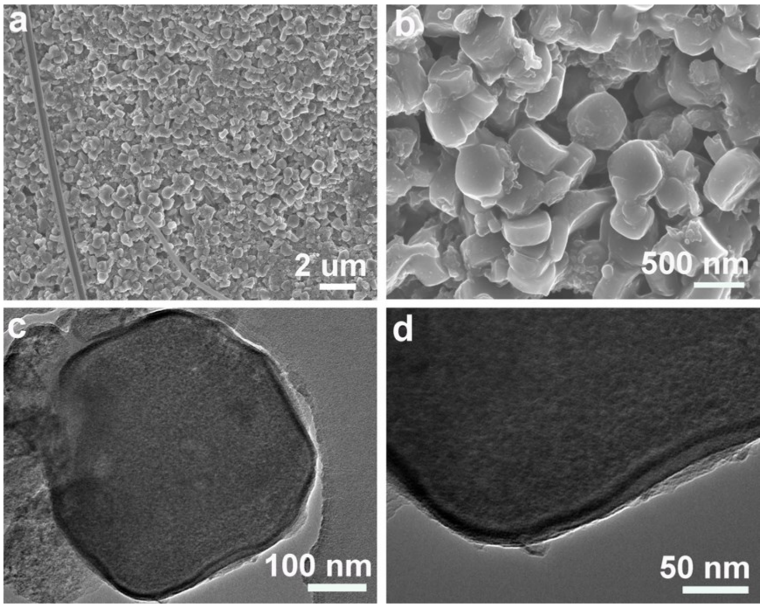

Fig. S5 Morphology characterization of TiO_2/C@NPSC-700 electrode after 2000 cycles at 1 A g^{-1}: (a, b) SEM images, (c, d) TEM images.

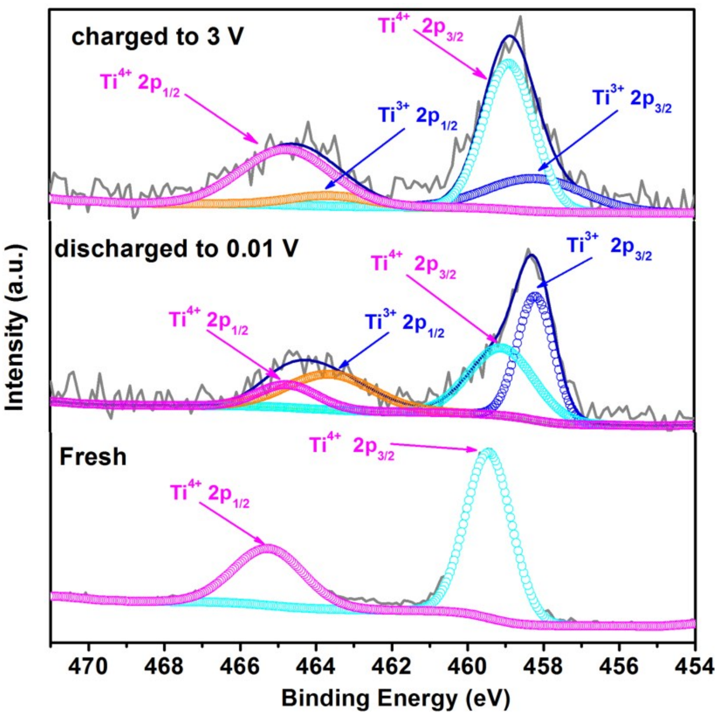

Fig. S6 Ti 2p spectra of TiO_2/C@NPSC-700 electrode at different charge/discharge states.

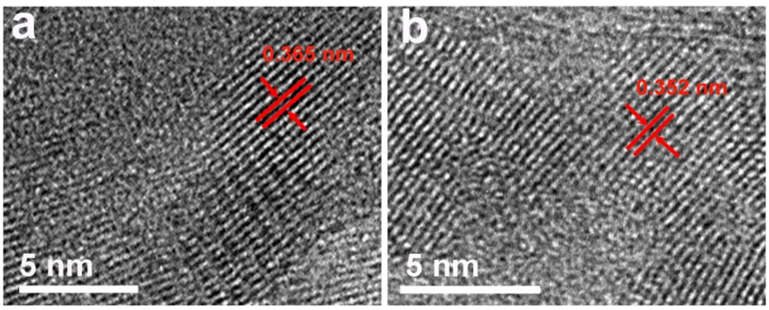

Fig. S7 HRTEM images of TiO_2/C@NPSC-700 electrode: (a) discarged to 0.01 V, (b) charged to 3 V.

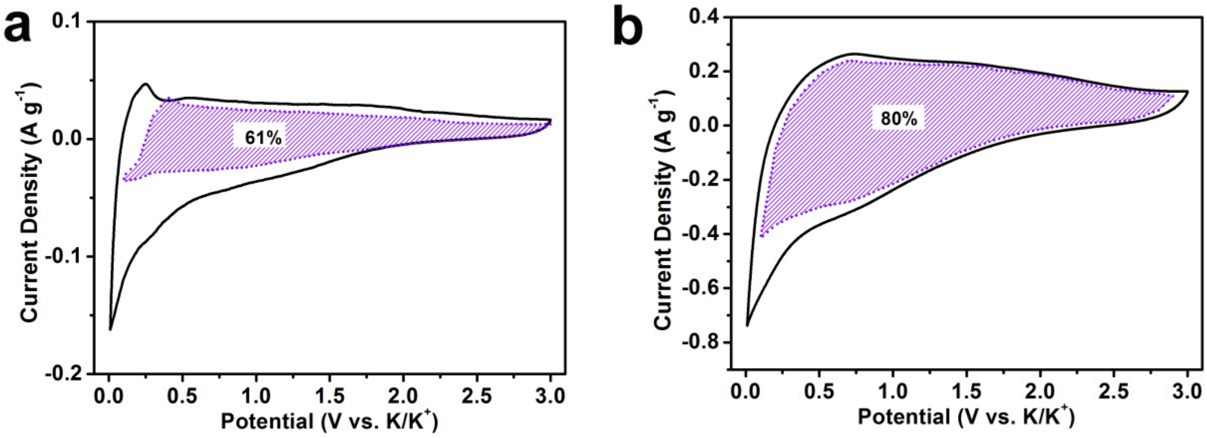

Fig. S8 The capacitive contribution at scan rate of (a) 0.1 mV s^{-1} and (b) 1 mV s^{-1}.

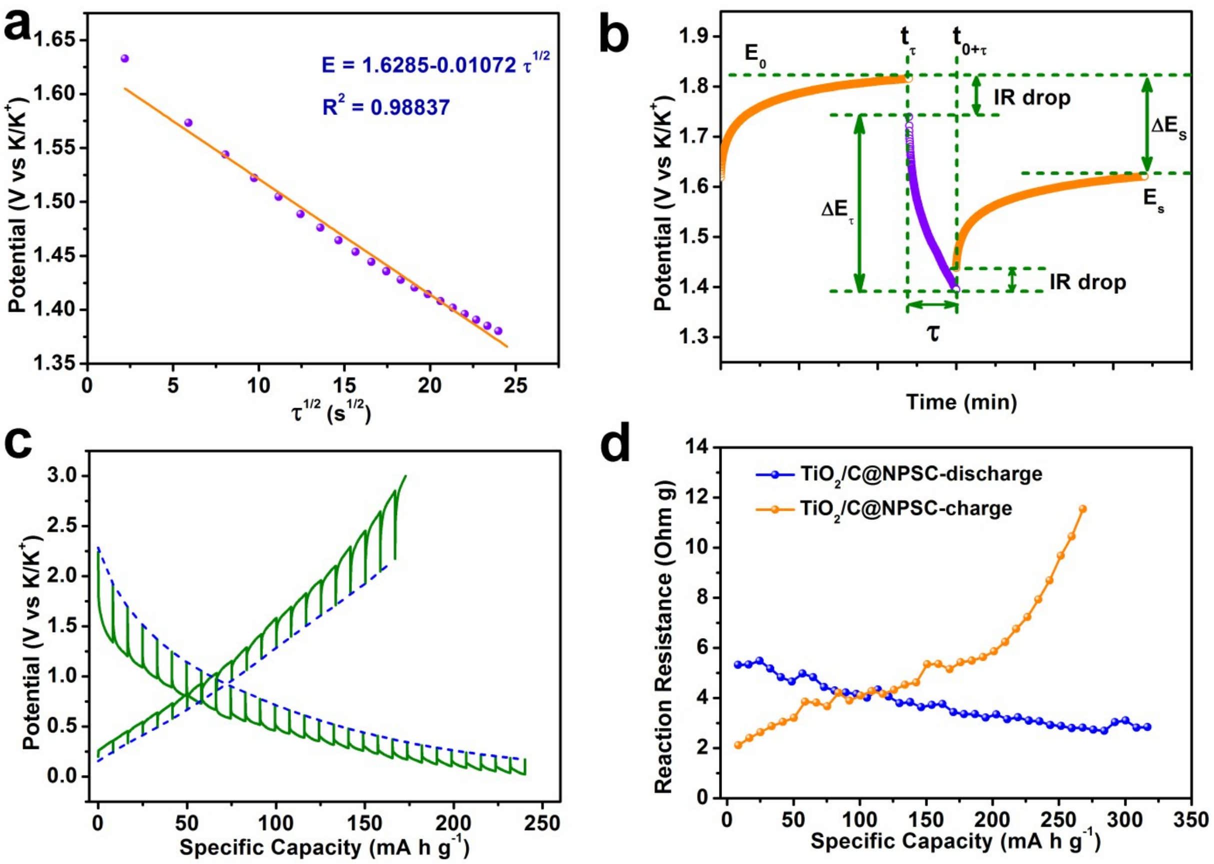

Fig. S9 (a) Variation of cell voltage during single titration plotted against $\tau^{1/2}$ for TiO_2/C@NPSC-700 anode, (b) Scheme for voltage response with time during a single constant current pulse. (c) GITT curves of TiO_2/C-700, (d) reaction resistance of TiO_2/C@NPSC-700 anode during GITT measurement.

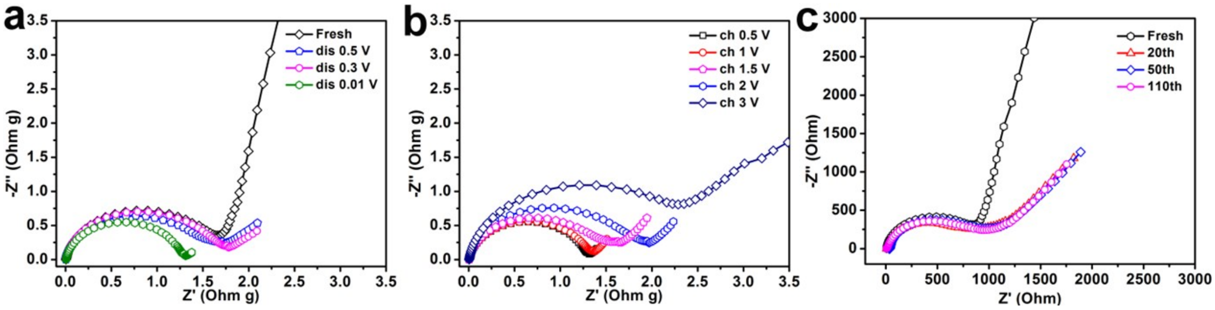

Fig. S10 EIS spectra of TiO_2/C@NPSC-700 anode at (a) different discharge states, (b) different charge states and (c) different cycles.

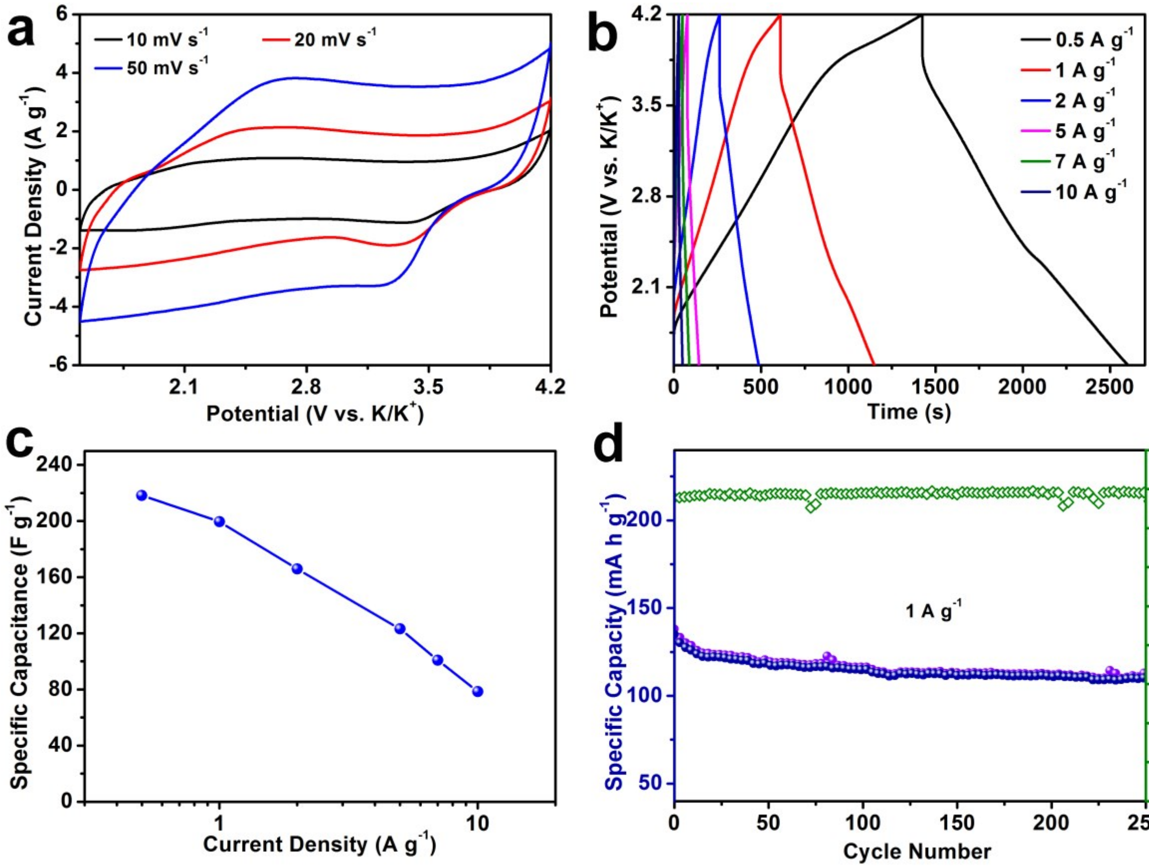

Fig. S11 Electrochemical performance of ZDPC electrode: (a) CV curves at different scan rates ranging from 10 to 50 mV s^{-1} under 1.5-4.2 V versus K/K^+, (b) GCD curves under different current densities ranging from 0.5 to 10 A g^{-1}, (c) the rate capability, and (d) the cycling performance and CE for 300 cycles at 1 A g^{-1}.

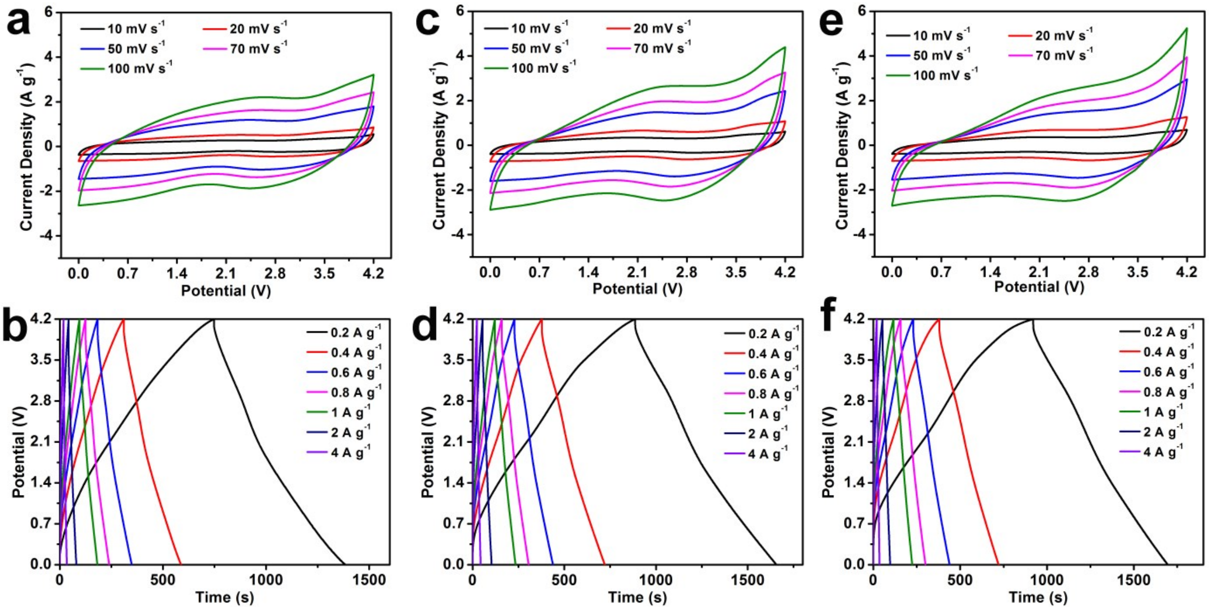

Fig. S12 Electrochemical performance of as-assembled PIHCs with different mass ratios of anode to cathode: (a) CV curves and (b) GCD profiles of PIHC with the mass ratio of 2:1; (c) CV curves and (d) GCD profiles of PIHC with the mass ratio of 1:1; (e) CV curves and (f) GCD profiles of PIHC with the mass ratio of 1:1.5.

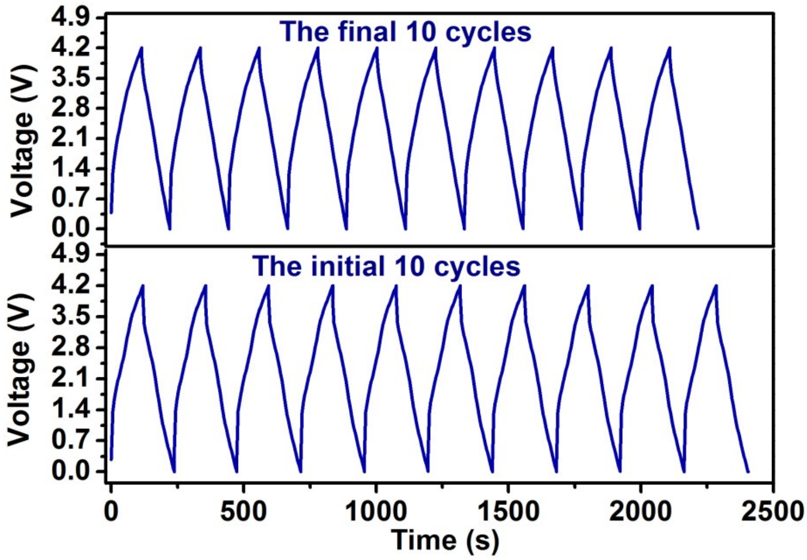

Fig. S13 The GCD profiles of the initial 10 cycles and the final 10 cycles.

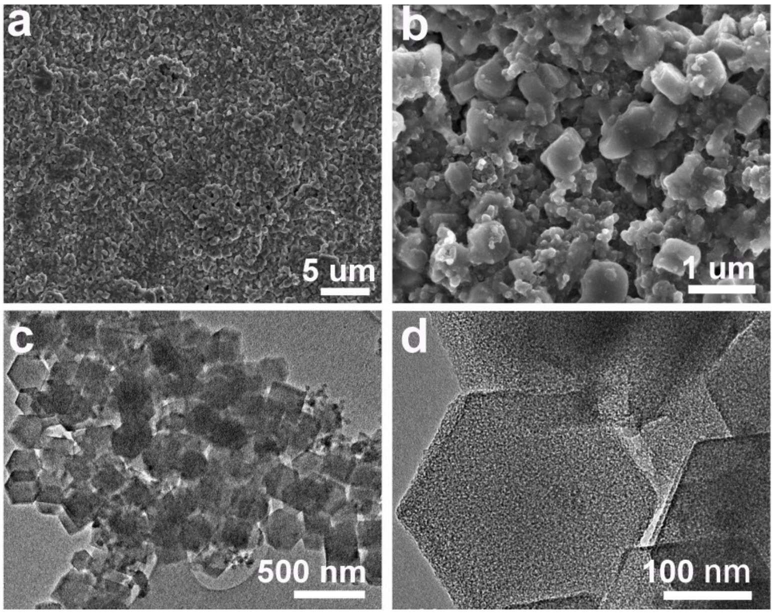

Fig. S14 (a-b) SEM images of TiO_2/C@NPSC-700 anode after 10 000 cycles in full-cell. (c-d) TEM images of ZDPC cathode after 10 000 cycles in full-cell.

Table S1. Physicochemical properties of different samples.

Samples	S_{BET} ($m^2\ g^{-1}$)	Pore volume ($cm^3\ g^{-1}$)	Pore size distribution (nm)	crystalline phases
MIL-125 (Ti)	1158.9	0.592	1.48-2.73, 7.40-252.57	
MIL-125 (Ti)@PZS	298.5	0.173	20.07-233.91	
TiO_2/C-700	275.8	0.171	1.48-5.04, 12.65-252.57	anatase
TiO_2/C@NPSC-600	51.7	0.041	1.48-2.73	anatase
TiO_2/C@NPSC-700	170.4	0.149	1.48-18.58	anatase
TiO_2/C@NPSC-800	274.5	0.212	1.48-11.72	anatase

Table S2. Composition date obtained from XPS investigation for the TiO_2/C@NPSC-x samples.

Samples	**Element content (at%)**					
	C	**N**	**O**	**P**	**S**	**Ti**
TiO_2/C@NPSC-600	69.95	1.82	18.89	6.55	1.02	1.77
TiO_2/C@NPSC-700	73.63	1.63	16.38	4.42	1.15	2.79
TiO_2/C@NPSC-800	77.55	1	14.56	3.12	0.55	3.22

Table S3. Comparison of the electrochemical performances of the as-prepared TiO_2/C@NPSC-700 anode with other anode materials for PIBs reported previously.

Electrode	Rate Capability (mA h g^{-1})/(A g^{-1})	Capacity Retention (%/cycles/current density)	ICE
TiO_2/C@NPSC (this work)	**309.5 mA h g^{-1}/0.05 A g^{-1}** **261 mA h g^{-1}/0.1 A g^{-1}** **221.8 mA h g^{-1}/0.2 A g^{-1}** **177.3 mA h g^{-1}/0.5 A g^{-1}** **142.4 mA h g^{-1}/1 A g^{-1}** **114.3 mA h g^{-1}/2 A g^{-1}**	**85%/5000 cycles/1 A g^{-1}**	**46.9%**
VSe_2 nanosheets[1]	374 mA h g^{-1}/0.1 A g^{-1} 350 mA h g^{-1}/0.2 A g^{-1} 334 mA h g^{-1}/0.5 A g^{-1} 269 mA h g^{-1}/1 A g^{-1} 172 mA h g^{-1}/2 A g^{-1}	87.3%/500 cycles/2 A g^{-1}	69.1%
VS_2[2]	380 mA h g^{-1}/0.1 A g^{-1} 250 mA h g^{-1}/1 A g^{-1} 100 mA h g^{-1}/2 A g^{-1}	No decay/100 cycles/0.5 A g^{-1}	—
TiO_2/RGO[3]	354.3 mA h g^{-1}/0.05 A g^{-1} 282.2 mA h g^{-1}/0.1 A g^{-1} 220.9 mA h g^{-1}/0.2 A g^{-1} 151.7 mA h g^{-1}/0.5 A g^{-1} 107.1 mA h g^{-1}/1 A g^{-1}	78%/200 cycles/0.2 A g^{-1} 85%/1000 cycles/1 A g^{-1}	35%
TiO_xN_y/C[4]	127 mA h g^{-1}/0.2 A g^{-1} 102 mA h g^{-1}/0.4 A g^{-1} 84 mA h g^{-1}/0.8 A g^{-1} 72 mA h g^{-1}/1.6 A g^{-1}	-/1250 cycles/0.2 A g^{-1}	—
PMC ($MoSe_2$/C)[5]	382 mA h g^{-1}/0.2 A g^{-1} 342 mA h g^{-1}/0.4 A g^{-1} 304 mA h g^{-1}/0.6 A g^{-1} 277 mA h g^{-1}/0.8 A g^{-1} 254 mA h g^{-1}/1 A g^{-1} 224 mA h g^{-1}/2 A g^{-1}	83.5%/1000 cycles/1 A g^{-1}	63.4%
CoP⊂NPPCS[6]	174 mA h g^{-1}/0.05 A g^{-1} 134 mA h g^{-1}/0.1 A g^{-1} 123 mA h g^{-1}/0.2 A g^{-1} 94 mA h g^{-1}/0.5 A g^{-1} 74 mA h g^{-1}/1 A g^{-1} 54 mA h g^{-1}/2 A g^{-1}	114 mA h g^{-1}/1000 cycles/0.5 A g^{-1}	19.6%

CoS@G[7]	530 mA h g^{-1}/0.1 A g^{-1} 414 mA h g^{-1}/0.5 A g^{-1} 365 mA h g^{-1}/1 A g^{-1} 310 mA h g^{-1}/2 A g^{-1} 278 mA h g^{-1}/3 A g^{-1} 232 mA h g^{-1}/4 A g^{-1}	70.2%/100 cycles/0.5 A g^{-1}	64.4%
V_2O_3@PNCNFs[8]	240 mA h g^{-1}/0.05 A g^{-1} 21 8 mA h g^{-1}/0.1 A g^{-1} 20 9 mA h g^{-1}/0.2 A g^{-1} 193 mA h g^{-1}/0.3 A g^{-1} 166 mA h g^{-1}/0.5 A g^{-1} 134 mA h g^{-1}/1 A g^{-1}	95.8%/500 cycles/0.05 A g^{-1}	60.3%
KTO/rGO[9]	228 mA h g^{-1}/0.1 A g^{-1} 162 mA h g^{-1}/0.2 A g^{-1} 116 mA h g^{-1}/0.5 A g^{-1} 84 mA h g^{-1}/1 A g^{-1} 75 mA h g^{-1}/2 A g^{-1}	—/700 cycles /2 A g^{-1}	24%
M-KTO[10]	105 mA h g^{-1}/0.1 A g^{-1} 81 mA h g^{-1}/0.3 A g^{-1}	51%/900 cycles/0.2 A g^{-1}	25.9%
a-Ti_3C_2 MNRs[11]	141 mA h g^{-1}/0.02 A g^{-1} 101 mA h g^{-1}/0.05 A g^{-1} 86 mA h g^{-1}/0.1 A g^{-1} 77 mA h g^{-1}/0.15 A g^{-1} 70 mA h g^{-1}/0.2 A g^{-1} 60 mA h g^{-1}/0.3 A g^{-1}	42 mA h g^{-1}/500 cycles/0.2 A g^{-1}	27%
HNTO/CS[12]	138.3 mA h g^{-1}/0.05 A g^{-1} 127.9 mA h g^{-1}/0.1 A g^{-1} 48.7 mA h g^{-1}/0.5 A g^{-1}	82.5%/1555 cycles /0.1 A g^{-1}	—
N-doped carbon nanofibers[13]	238 mA h g^{-1}/0.1 A g^{-1} 217 mA h g^{-1}/0.2 A g^{-1} 192 mA h g^{-1}/0.5 A g^{-1} 172 mA h g^{-1}/1 A g^{-1} 153 mA h g^{-1}/2 A g^{-1} 126 mA h g^{-1}/5 A g^{-1} 104 mA h g^{-1}/10 A g^{-1} 101 mA h g^{-1}/20 A g^{-1}	146 mA h g^{-1}/4000 cycles/2 A g^{-1}	49%
HINCA[14]	342.8 mA h g^{-1}/0.028 A g^{-1} 302.8 mA h g^{-1}/0.056 A g^{-1} 251.4 mA h g^{-1}/0.14 A g^{-1} 200 mA h g^{-1}/0.28 A g^{-1} 114.3 mA h g^{-1}/0.56 A g^{-1}	0.05% decay/per cycle/500 cycles/0.14 A g^{-1}	72.1%

CNFF[15]	240 mA h g^{-1}/0.05 A g^{-1} 236 mA h g^{-1}/0.08 A g^{-1} 214 mA h g^{-1}/0.1 A g^{-1} 202 mA h g^{-1}/0.2 A g^{-1} 181 mA h g^{-1}/0.5 A g^{-1} 164 mA h g^{-1}/1 A g^{-1}	0.006% decay/per cycle/2000 cycles /1 A g^{-1}	—

Table S4. Electrochemical performance comparison of as-assembled TiO_2/C@NPSC//ZDPC PIHC with other PIHC, SIHCs and LIHCs reported early.

System	Energy density/Power density	Potential Window (V)	Capacity Retention/current density/Cycling life
PIHCs			
Our work	**114 W h kg^{-1}/210 W kg^{-1}** **37.3 W h kg^{-1}/21 kW kg^{-1}**	**0-4.2**	**91.6%/1 A g^{-1}/10 000 cycles**
CTP@//AC[16]	80 W h kg^{-1}/32 W kg^{-1} 34 W h kg^{-1}/5.144 kW kg^{-1}	1-4	75.9%/5 A g^{-1}/4000 cycles
Soft carbon//AC[17]	120 W h kg^{-1}/96 W kg^{-1} 4.32 W h kg^{-1}/0.536 kW kg^{-1}	0-4	97.5%/0.75 A g^{-1} /1500 cycles
KTO//NGC[18]	58.2 W h kg^{-1}/160 W kg^{-1} 11.8 W h kg^{-1}/7.2 kW kg^{-1}	0-3.5	75.5%/1 A g^{-1}/5000 cycles
CO_2P@rGO//AC[19]	87 W h kg^{-1}/12 W kg^{-1} 10 W h kg^{-1}/4.2647 kW kg^{-1}	1-4	68%/1 A g^{-1}/1000 cycles
NHCS//ANHCS[20]	114.2 W h kg^{-1}/100.5 W kg^{-1} 19.1 W h kg^{-1}/8.203 kW kg^{-1}	0.01-4	93%/0.5 A g^{-1}/2000 cycles 80.4%/2 A g^{-1}/5000 cycles
S-N-PCNs//AC[21]	187 W h kg^{-1}/99 W kg^{-1} 76 W h kg^{-1}/5.136 kW kg^{-1}	0-4	86.4%/1 A g^{-1}/3000 cycles
SIHCs			
HP-CNWs//FM-CNSs[22]	130.6 W h kg^{-1}/210 W kg^{-1} 43.6 W h kg^{-1}/15.26 kW kg^{-1}	0.5-4.2	85.4%/0.5 A g^{-1}/3000 cycles
MWTOG//AC[23]	64.2 W h kg^{-1}/56.3 W kg^{-1} 25.8 W h kg^{-1}/1.357 kW kg^{-1}	1-3.8	90%/3.35 A g^{-1}/10 000 cycles
Gr-Nb_2O_5//AC[24]	112.9 W h kg^{-1}/80.1 W kg^{-1} 62.2 W h kg^{-1}/5.33 kW kg^{-1}	1-4.3	97.1%/1 A g^{-1}/1500 cycles
TiO_2@CNT@C//BAC[25]	81.2 W h kg^{-1}/126 W kg^{-1} 37.9 W h kg^{-1}/12.4 kW kg^{-1}	1-4	85.5/1 A g^{-1}/5000 cycles
N-TiO_2//AC[26]	80.3 W h kg^{-1}/500 W kg^{-1} 24.6 W h kg^{-1}/12.5 kW kg^{-1}	1-4	85%/1 A g^{-1}/6500 cycles
PSNC//PSOC-A[27]	201 W h kg^{-1}/185 W kg^{-1} 50 W h kg^{-1}/16.5 kW kg^{-1}	1.5-3.5	72%/6.4 A g^{-1}/10 000 cycles
LIHCs			
MoO_2-CNT//AC [28]	70 W h kg^{-1}/83 W kg^{-1} 34 W h kg^{-1}/4 kW kg^{-1}	0.8-3.2 V	75%/1000 cycles/1 A g^{-1}

Co_3ZnC@NC//MPC[29]	141.4 W h kg^{-1}/275 W kg^{-1} 15.2 W h kg^{-1}/10.3 kW kg^{-1}	1-4.5	80%/ 1 A g^{-1}/1000 cycles
Nb_2O_5//AC[30]	95.55 W h kg^{-1}/191 W kg^{-1} 65.39 W h kg^{-1}/5.35 kW kg^{-1}	1-3.5 V	83%/1000 cycles/2.2 A g^{-1}
TiC//PHPNC[31]	101.5 W h kg^{-1}/450 W kg^{-1} 23.4 W h kg^{-1}/67.5 kW kg^{-1}	0-4.5 V	82%/5000 cycles/2 A g^{-1}

References:

1. C. Yang, J. Feng, F. Lv, J. Zhou, C. Lin, K. Wang, Y. Zhang, Y. Yang, W. Wang, J. Li and S. Guo, *Adv. Mater.*, 2018, **30**, 1800036.
2. J. Zhou, L. Wang, M. Yang, J. Wu, F. Chen, W. Huang, N. Han, H. Ye, F. Zhao, Y. Li and Y. Li, *Adv. Mater.*, 2017, **29**, 1702061.
3. Y. Fang, R. Hu, B. Liu, Y. Zhang, K. Zhu, J. Yan, K. Ye, K. Cheng, G. Wang and D. Cao, *J. Mater. Chem. A*, 2019, **7**, 5363-5372.
4. M. Tao, G. Du, Y. Zhang, W. Gao, D. Liu, Y. Luo, J. Jiang, S. Bao and M. Xu, *Chem. Eng. J.*, 2019, **369**, 828-833.
5. W. Wang, B. Jiang, C. Qian, F. Lv, J. Feng, J. Zhou, K. Wang, C. Yang, Y. Yang and S. Guo, *Adv. Mater.*, 2018, **30**, 1801812.
6. J. Bai, B. Xi, H. Mao, Y. Lin, X. Ma, J. Feng and S. Xiong, *Adv. Mater.*, 2018, **30**, 1802310.
7. H. Gao, T. Zhou, Y. Zheng, Q. Zhang, Y. Liu, J. Chen, H. Liu and Z. Guo, *Adv. Funct. Mater.*, 2017, **27**, 1702634.
8. T. Jin, H. Li, Y. Li, L. Jiao and J. Chen, *Nano Energy*, 2018, **50**, 462-467.
9. C. Zeng, F. Xie, X. Yang, M. Jaroniec, L. Zhang and S. Qiao, *Angew. Chem., Int. Ed. Engl.* 2018, **57,** 8540-8544.
10. Y. Dong, Z. S. Wu, S. Zheng, X. Wang, J. Qin, S. Wang, X. Shi and X. Bao, *ACS Nano*, 2017, **11**, 4792-4800.
11. P. Lian, Y. Dong, Z.-S. Wu, S. Zheng, X. Wang, W. Sen, C. Sun, J. Qin, X. Shi and X. Bao, *Nano Energy*, 2017, **40**, 1-8.
12. P. Li, W. Wang, S. Gong, F. Lv, H. Huang, M. Luo, Y. Yang, C. Yang, J. Zhou, C. Qian, B. Wang, Q. Wang and S. Guo, *ACS Appl. Mater. interfaces*, 2018, **10**, 37974-37980.
13. Y. Xu, C. Zhang, M. Zhou, Q. Fu, C. Zhao, M. Wu and Y. Lei, *Nat. Commun.*, 2018, **9**, 1720.
14. D. S. Bin, X. J. Lin, Y. G. Sun, Y. S. Xu, K. Zhang, A. M. Cao and L. J. Wan, *J. Am. Chem. Soc.*, 2018, **140**, 7127-7134.
15. H. Li, Z. Cheng, Q. Zhang, A. Natan, Y. Yang, D. Cao and H. Zhu, *Nano Lett.*, 2018, **8**, 7407-7413.
16. Z. Zhang, M. Li, Y. Gao, Z. Wei, M. Zhang, C. Wang, Y. Zeng, B. Zou, G. Chen and F. Du, *Adv. Funct. Mater.*, 2018, **28**, 1802684.
17. L. Fan, K. Lin, J. Wang, R. Ma and B. Lu, *Adv. Mater.*, 2018, **30**, 1800804.
18. S. Dong, Z. Li, Z. Xing, X. Wu, X. Ji and X. Zhang, *ACS Appl. Mater. interfaces*, 2018, **10**, 15542-15547.
19. Y. Wang, Z. Zhang, G. Wang, X. Yang, Y. Sui, F. Du and B. Zou, *Nanoscale Horiz.*, 2019, **4**, 1394-1401.
20. D. Qiu, J. Guan, M. Li, C. Kang, J. Wei, Y. Li, Z. Xie, F. Wang and R. Yang, *Adv. Funct. Mater.*, 2019, **29**, 1903496.
21. X. Hu, Y. Liu, J. Chen, L. Yi, H. Zhan and Z. Wen, *Adv.Energy Mater.*, 2019, **9**, 1901533.
22. M. Y. Song, N. R. Kim, S. Y. Cho, H.-J. Jin and Y. S. Yun, *ACS Sustainable Chem. Eng.*, 2017, **5**, 616-624.
23. Z. Le, F. Liu, P. Nie, X. Li, X. Liu, Z. Bian, G. Chen, H. B. Wu and Y. Lu, *ACS Nano*, 2017, **11**, 2952-2960.
24. X. Wang, Q. Li, L. Zhang, Z. Hu, L. Yu, T. Jiang, C. Lu, C. Yan, J. Sun and Z. Liu, *Adv. Mater.*, 2018, **30**, e1800963.
25. Y.-E. Zhu, L. Yang, J. Sheng, Y. Chen, H. Gu, J. Wei and Z. Zhou, *Adv. Energy Mater.*, 2017, **7**, 1701222.
26. S. Liu, Z. Cai, J. Zhou, A. Pan and S. Liang, *J. Mater. Chem. A*, 2016, **4**, 18278-18283.
27. J. Ding, H. Wang, Z. Li, K. Cui, D. Karpuzov, X. Tan, A. Kohandehghan and D. Mitlin, *Energy Environ. Sci.*, 2015, **8**, 941-955.
28. S. Fleischmann, M. Zeiger, A. Quade, A. Kruth and V. Presser, *ACS Appl. Mater. interfaces*, 2018, **10**, 18675-18684.
29. G. Zhu, T. Chen, L. Wang, L. Ma, Y. Hu, R. Chen, Y. Wang, C. Wang, W. Yan, Z. Tie, J. Liu and Z. Jin, *Energy Storage Mater.*, 2018, **14**, 246-252.
30. B. Deng, T. Lei, W. Zhu, L. Xiao and J. Liu, *Adv. Funct. Mater.*, 2018, **28**, 1704330.
31. H. Wang, Y. Zhang, H. Ang, Y. Zhang, H. T. Tan, Y. Zhang, Y. Guo, J. B. Franklin, X. L. Wu, M. Srinivasan, H. J. Fan and Q. Yan, *Adv. Funct. Mater.*, 2016, **26**, 3082-3093.